ELSEVIER

Polymer 41 (2000) 4179–4187

polymer

Segmented liquid-crystalline polyesters with allyl groups as lateral substituents. Synthesis and characterization

D. Acierno[a], R. Fresa[b], P. Iannelli[b,*], P. Vacca[b]

[a]*Dipartimento di Ingegneria dei Materiali e della Produzione, Università di Napoli, P. le Tecchio, I-80125 Napoli, Italy*
[b]*Dipartimento di Ingegneria Chimica ed Alimentare, Università di Salerno, via Ponte Don Melillo, I-84084 Fisciano, Salerno, Italy*

Received 26 March 1999; received in revised form 2 July 1999; accepted 2 September 1999

Abstract

The synthesis and the characterization of segmented liquid-crystalline [**P**(*n*)] made by interfacial polycondensation of 3-allyl-4,4′-dihydroxybiphenyl and the acid chlorides of α,ω-dicarboxy-alkanes are reported. The flexible spacers contain even numbers of methylene units ($n = 6$–14). All polymers are enantiotropic showing a nematic phase with isotropization temperature in the range of about 95–175°C. At room temperature all polymers show a mesophasic structure except for **P**(8) which is crystalline. Both **P**(12) and **P**(14) show a quasi-hexagonal phase with six chains per unit cell.

Keywords: Liquid-crystalline polymers; Network; X-ray diffraction

1. Introduction

Recently we have reported the synthesis of a new class of main-chain liquid-crystalline polymers (LCPs) bearing lateral substituents with carbon–carbon unsaturation [1–3]. Due to the relatively high thermal stability of the unsaturation, these polymers may be processed to give oriented products, which may undergo crosslinking. In this way macro-oriented networks (LCNs) are prepared in which sample morphology is frozen and anisotropy is preserved even at high temperatures [1,4]. By coupling the effect of lateral substituents in the polymeric chain (which increase processability by decreasing the melting temperature) with crosslinking, these novel materials are promising in those applications where anisotropy is required, like the case of high tensile/compressive performance and nonlinear optics. For instance, fiber samples of the polymer with formula

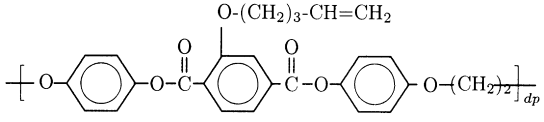

were crosslinked by thermally activated radical reaction to give highly oriented networks with a tensile modulus of about 11 GPa at room temperature and 3.5 GPa at 150°C (at this temperature the virgin material is in the liquid-crystalline state) [1]. Similar results were obtained [4] by exposing to moderate doses of γ-radiation fiber samples of polymers **PA**(*n*) with formula

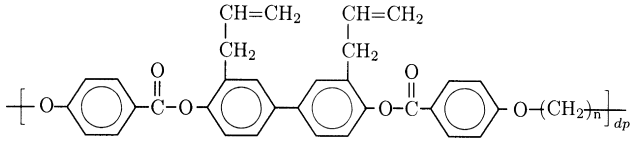

PA(n) n=6,8,10,12

Many authors have proposed different approaches to synthesize oriented LCNs, mainly of the side-chain type [5–11]. Noteworthy is the path suggested by Finkelman [7,8] and by Ober [9] who proposed a two step process: first a prepolymerization is carried out, then a final crosslinking is performed with mechanical stress applied to the sample. In this way densely crosslinked LCNs with the molecular structure feature of a smectic phase showing interesting mechanical performance have been obtained. While this approach is suitable for basic investigation, it is not applicable for manufacturing on a large scale. In this case the procedure we reported seems to be promising, provided that both thermal stability of raw material and easy promotion of crosslinking are ensured.

With the aim of selecting new monomers bearing unsaturation to be used for easy-to-make LCNs, in this paper we

* Corresponding author.
E-mail address: Iannelli@dica.unisa.it (P. Iannelli).

0032-3861/00/$ - see front matter
PII: S0032-3861(99)00634-5

Table 1
Thermodynamic DSC data concerning untreated fibers of polymers **P**(*n*)

Polymer	T_m[a]	ΔH_m[b]	T_i[c]	ΔH_i[d]	M_w[e] ($\times 10^3$)	P_i[f]	η[g]
P(6)	–	–	172.7	13.1	43	2.7	0.67
P(8)	118.6	24.3	141.2	14.3	145	2.0	1.19
P(10)	–	–	111.6	14.6	44	2.1	0.72
P(12)	–	–	103.7	13.3	42	2.9	0.94
P(14)	69.5	3.0	94.0	15.6	36	2.0	0.61
			(76.8)[h]	(1.6)[h]			

[a] T_m (°C), melting temperature.
[b] ΔH_m (J/g), melting enthalpy.
[c] T_i (°C), isotropization temperature.
[d] ΔH_i (J/g), isotropization enthalpy. Temperatures are measured at the maximum of the transition endotherm.
[e] Weight average molecular weight obtained by GPC, polystyrene as standard.
[f] Polydispersity index.
[g] η (dl/g), intrinsic viscosity measured at 25.0°C in chloroform.
[h] Reversible endotherm for **P**(14) which may be ascribed to a smectic–nematic transition.

report the synthesis and characterization of a set of polymers with formula:

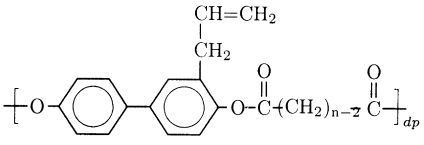

P(n) n=6,8,10,12,14

The phase behavior of crosslinked derivatives will appear in a forthcoming article.

2. Experimental

Fibers were extruded from the anisotropic liquid phase and cooled without temperature control. Thermal measurements were carried out on fiber samples by means of a DSC-7 Perkin–Elmer calorimeter under nitrogen flow at 10°C/min rate. Optical microscopy was performed by means of a Jenapol microscope fitted with a Linkam THMS 600 hot stage. Fiber diffraction spectra were recorded under vacuum by means of a cylindrical camera with a radius of 57.3 mm and the X-ray beam (V-filtered Cr-Kα radiation) direction perpendicular to the fiber axis. The high temperature X-ray diffraction patterns were collected using a flat camera and a modified Linkam THMS 600 hot stage. The ^{1}H NMR spectra were recorded in $CDCl_3$ solution with a Bruker DRX/400 Spectrometer. Chemical shifts are reported relative to the residual solvent peak ($CHCl_3$: $\delta_H = 7.26$). For GPC analysis a Waters 150-C ALC/GPC instrument was employed, equipped with four 300×7.5 mm^2 columns type PL Gel MIXED A 20 μ and a Jasco 875 UV detector set at 254 nm (polystyrene as standard and chloroform as solvent,

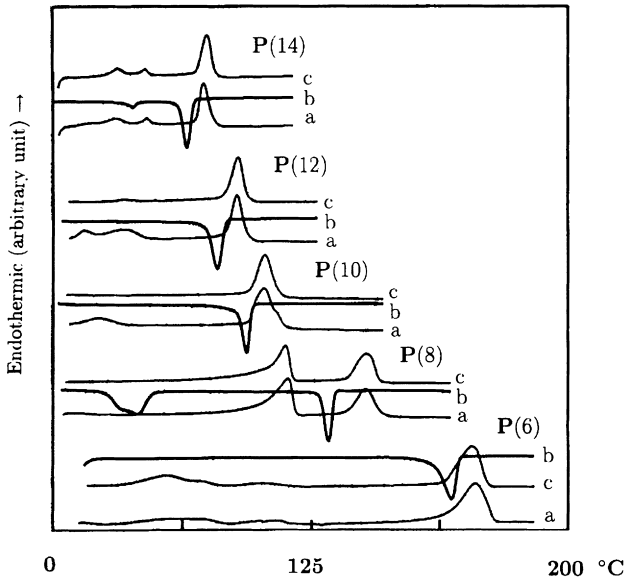

Fig. 1. (a) First heating; (b) first cooling; and (c) second heating DSC traces of virgin fibers of **P**(*n*).

at 1 ml/min and 30°C). Solution viscosity measurements (Ubbelohde viscometer) were performed in chloroform at 25.0 ± 0.1°C.

2.1. Synthesis of precursors

All reagents were used as obtained from Aldrich. Polymers **P**(*n*) were synthesized by the interfacial polycondensation reaction of 3-allyl-4,4′-dihydroxybiphenyl (**1**) and the acid chloride of the appropriate α,ω-dicarboxy-*n*-alkane.

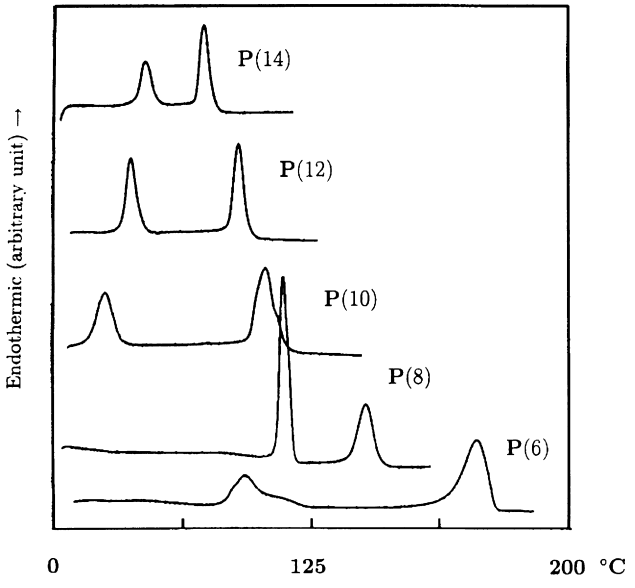

Fig. 2. First DSC heating traces of annealed fiber samples of **PA**(*n*), according to Table 2.

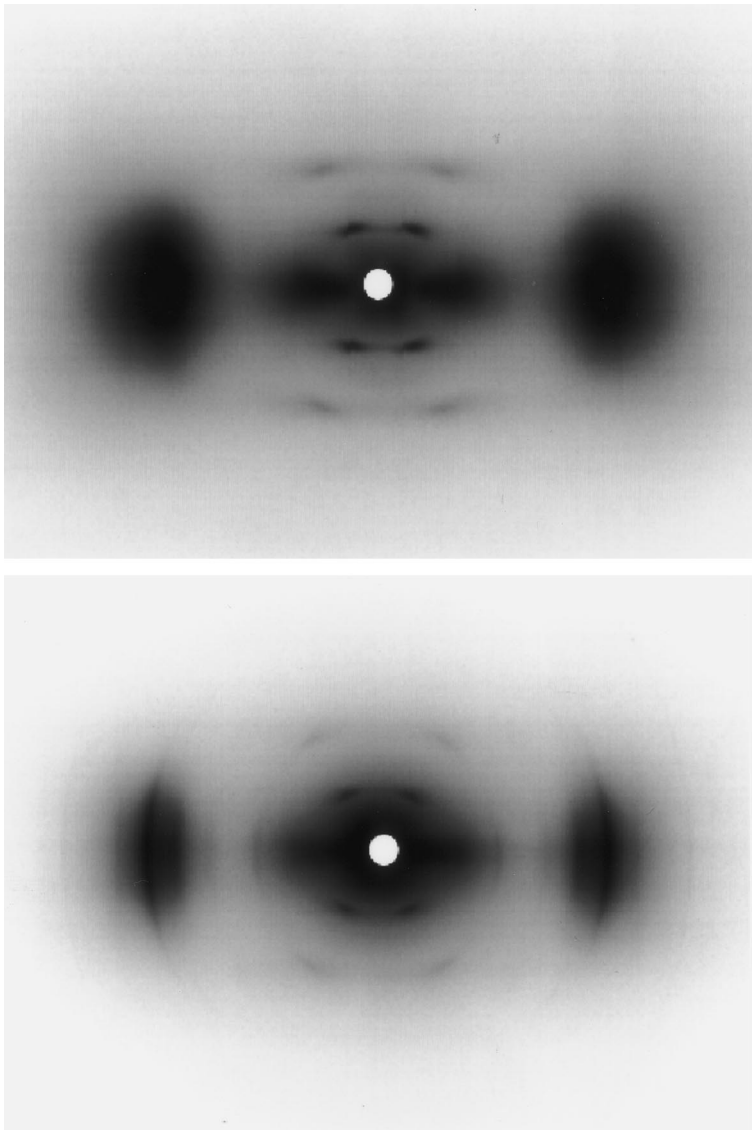

Fig. 3. X-ray fiber diffraction patterns at room temperature of **P**(6): virgin (top) and annealed (bottom) fiber sample.

Table 2
Thermodynamic DSC data concerning untreated fibers of polymers**P**(*n*) (temperatures are measured at the maximum of the transition endotherm, all fibers have been annealed for 2.5 h)

Polymer	T_t [a]	T_m [b]	ΔH_m [c]	T_l [d]	ΔH_i [e]
P(6)	90	105.8	7.6	173.5	15.4
P(8)	110	117.0	18.0	142.6	14.0
P(10)	50	65.2	7.0	111.9	13.4
P(12)	60	72.5	12.4	104.1	14.3
P(14)	65	76.5	10.0	93.8	15.3

[a] T_t (°C), annealing temperature.
[b] T_m (°C), melting temperature.
[c] ΔH_m (J/g), melting enthalpy.
[d] T_i (°C), isotropization temperature.
[e] ΔH_i (J/g), isotropization enthalpy.

Compound **1** was obtained by reaction of 4,4′-dihydroxybiphenyl with allyl bromide followed by Claisen transposition. First 50.0 g of 4,4′-dihydroxybiphenyl was dissolved in 300 cm^3 of boiling ethanol and 50 cm^3 of water with 18.0 g of KOH, then the equimolar amount of allyl bromide (32.5 g) was added dropwise. After 1 h of reaction, the precipitated crystalline phase of 4,4′-diallyloxy-biphenyl was separated by filtration and the solution was treated with hydrochloric acid until complete precipitation of 4-allyloxy-4′-hydroxybiphenyl. Purification was performed by crystallization from chloroform/heptane solution. The white crystalline material was collected, washed for several minutes with heptane, then filtered and dried in an oven (T_m = 170°C—yield 25%). Following the Claisen transposition procedure [12], this compound was kept at 240°C under argon for 30 min to obtain **1**, which was crystallized by cooling at room temperature and purified by

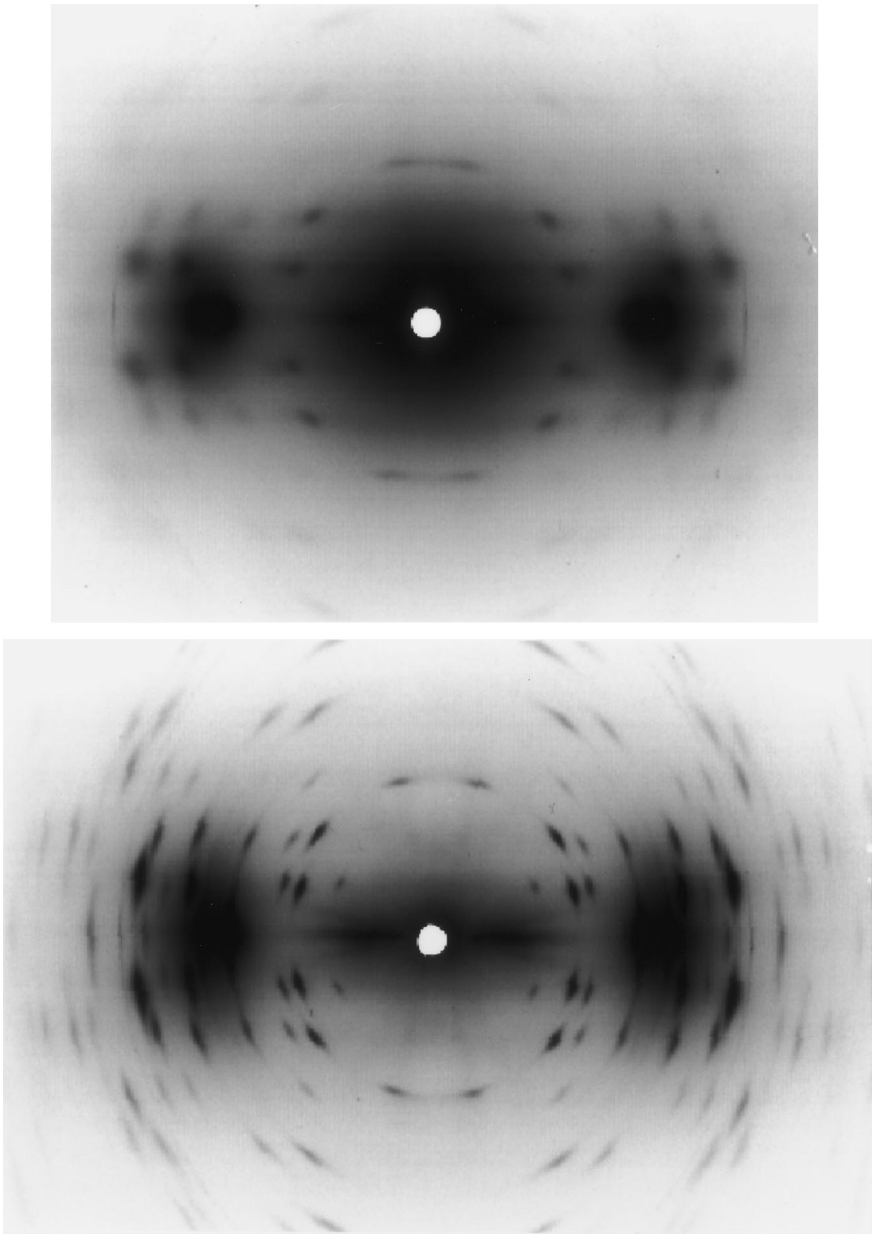

Fig. 4. X-ray fiber diffraction patterns at room temperature of **P**(8): virgin (top) and annealed (bottom) fiber sample.

crystallization from boiling *n*-octane. Further purification was performed by sublimation under vacuum (T_m = 107.3°C, ΔH = 114 J/g—yield 70%). Proton resonance data at 25°C (chloroform as solvent) are:

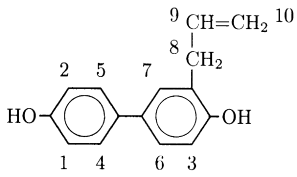

^{1}H NMR [δ (ppm), 1–3 (6.9,m); 4,5 (7.4,d); 6,7 (7.3,m); 8 (3.5,d); 9 (6.0,m); 10 (5.2,m)].

Acid chloride formation from α,ω-dicarboxy-*n*-alkanes was performed by refluxing with thionyl chloride and distillation under vacuum.

2.2. Polymer synthesis

Approximately 1.5 g of **1** was dissolved in 100 cm^3 of water with 3% excess of KOH and 0.700 g of benzyltriethylammonium chloride. The equimolar amount of the appropriate chloride was dissolved in 50 cm^3 of chloroform previously treated with aluminum oxide. The two solutions were stirred vigorously in a blender for 8 min. The polymer was precipitated by addition of *n*-heptane (100–150 cm^3) and, after filtration, washed three times with a chloroform/heptane (30/70 v/v)

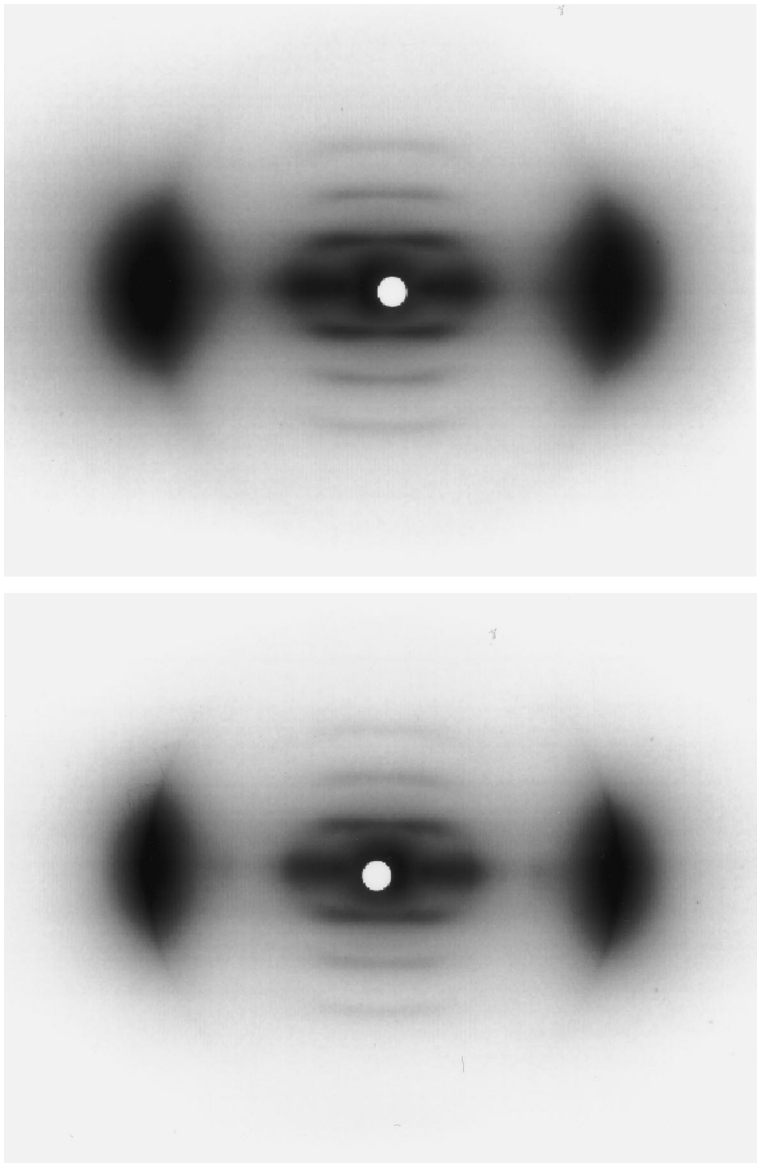

Fig. 5. X-ray fiber diffraction patterns at room temperature of **P**(10): virgin (top) and annealed (bottom) fiber sample.

solution, once with 95% ethanol, and three times with water. Finally, the polymer was oven dried at 60°C under vacuum.

Proton resonance data at 25°C (chloroform as solvent) are:

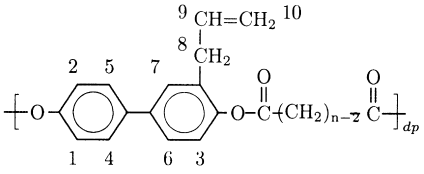

^{1}H NMR [δ (ppm), 1–3 (7.1,m); 4,5 (7.5,d); 6,7 (7.4,m); 8 (3.3,d); 9 (5.9,m); 10 (5.1,m); methylene units starting from carbonyl: first 2.7, second 1.9, other ones 1.5)]. Extrapolated intrinsic viscosities and molecular weights by GPC are given in Table 1.

3. Results and discussion

3.1. Thermal analysis

The DSC traces of virgin as well as annealed fiber samples of **P**(*n*) are shown in Figs. 1 and 2 while the corresponding thermodynamic data are given in Tables 1 and 2 respectively. **P**(*n*) are thermotropic LCPs of nematic type according to optical microscopy and to the X-ray diffraction pattern recorded within the thermal stability range of the LC phase (equatorial halo peaked at $\sin\theta/\lambda = 0.11$ Å^{-1} and no Bragg diffraction for lattice distances lower than ≈ 41 Å). **P**(14) shows a small reversible peak at 76.8°C (Fig. 1) which may be ascribed to a smectic–nematic transition according to the undercooling of only 7°C in the cooling run. X-ray measurements as a function of temperature for confirming

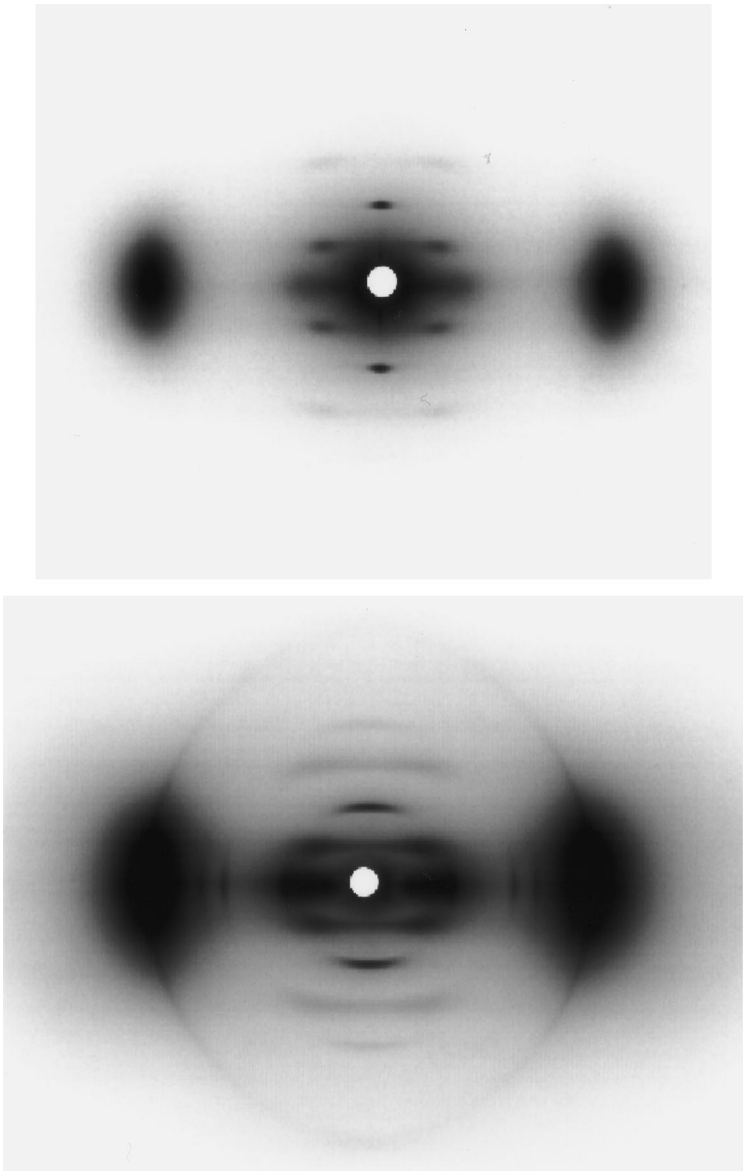

Fig. 6. X-ray fiber diffraction patterns at room temperature of **P**(12): virgin (top) and annealed (bottom) fiber sample.

this hypothesis were not possible because of the thermodynamic instability of the smectic phase.

Thermal behavior is completely reversible and crosslinking does not occur even after annealing at 130°C for 30 min, the samples being still fully soluble in chloroform at room temperature.

Compared to the analogous class of polymers with the biphenyl unit with no allyl group [13–15], reported to show a smectic S_H phase [13], the isotropization temperatures of **P**(*n*) are much lower due to the combined effect of lateral substituent and the random insertion of allyl–biphenyl units (*head-to-head* and *head-to-tail*) along the chain [from Ref. [13]—$n = 8:\ T_m = 240°C,\ T_i = 336°C;\ n = 10:\ T_m = 227°C, T_i = 290°C; n = 12: T_m = 203°C, T_i = 253°C; n = 14:\ T_m = 194°C,\ T_i = 237°C$]. For the same reason the crystalline state is restrained, except for **P**(8) as will be discussed in the following section.

3.2. X-ray diffraction analysis

The mesophasic nature of the phases stable at room temperature is clearly shown by the X-ray diffraction pattern of fiber samples (Figs. 3–7). Annealing induces some structural modification in the solid state and the lack of orientation to some extent. Only **P**(8) shows a crystalline phase to which corresponds a diffraction pattern rich in reflections. It is worth noting that all phases are different from each other ranging from a smectic C phase for $n = 6$ to a quasi-hexagonal phase for $n = 12, 14$. Keeping in mind that with the exception of **P**(8) all phases are mesophasic rather than

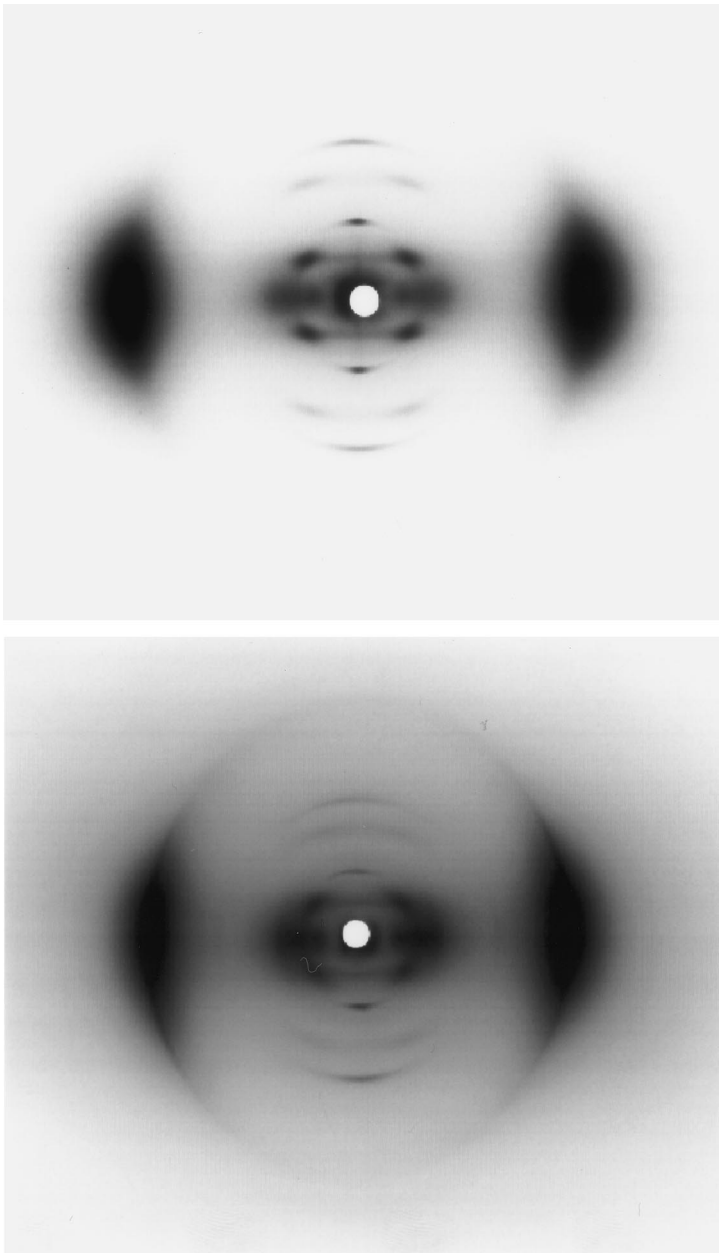

Fig. 7. X-ray fiber diffraction patterns at room temperature of **P**(14): virgin (top) and annealed (bottom) fiber sample.

crystalline thus strong packing distortion is present, coarse cell parameters are given in Table 3. In all cases the *c* axis is equal to the length of the monomeric unit in its most extended conformation.

3.2.1. **P***(6)*

Fiber sample shows a smectic C phase with a tilting angle of about 26° (Fig. 3). Annealing increases the sharpness of the strong equatorial peak ($d = 4.29$) and promotes the appearance of four more weak equatorial reflections with lattice spacing of 8.03 Å (sharp), 5.87 Å (very weak, broad), 4.89 Å (broad), and 3.81 Å (sharp). The crystalline state is not well developed, especially for the chain-to-chain transverse registers (no out of meridian reflections). Indeed the very low annealing temperature, which must be kept lower than the melting one, might not be effective in promoting adequate chain mobility in the solid state and then crystallization. Except for **P**(8), this limitation occurs for all the polymers.

3.2.2. **P***(8)*

The phase stable at room temperature is crystalline. Crystallinity is improved by annealing (Fig. 4). Adopting the hypothesis that the diffraction spots closest to the meridian in Fig. 4 are the 00*l* reflections, the triclinic unit cell with lattice parameters $a = 9.62$ Å, $b = 8.92$ Å, $c = 20.2$ Å, $\alpha =$

Table 3
Type of phases observed for virgin and annealed fibers of polymers **P**(*n*)

Polymer	T_t[a]	Type of phase	
P(6)		Smectic C (tilting angle = 29°, c = 16.8 Å)	Fig. 3—top
P(6)	90	As above plus some more equatorial reflections	Fig. 3—bottom
P(8)		Crystalline (c = 20.2 Å)	Fig. 4—top
P(8)	110	Crystalline with cell parameters a = 9.62 Å, b = 8.92 Å, c = 20.2 Å α = 107.8°, β = 90.0°, γ = 81.0°	Fig. 4—bottom
P(10)		Mesophase (c = 22.5 Å)	Fig. 5—top
P(10)	50	As above but with sharper equatorial reflection	Fig. 5—bottom
P(12)		Smectic A type mesophase (c = 24.5/25.3 Å)	Fig. 6—top
P(12)	60	Quasi-hexagonal phase with cell parameters $a = b$ = 12.79 Å, γ = 60°, c = 24.5/25.3 Å (d = 1.29 g/cm^3)	Fig. 6—bottom
P(14)		Mesophase (c = 26.8/27.6 Å)	Fig. 7—top
P(14)	65	Quasi-hexagonal phase with cell parameters $a = b$ = 12.9 Å, γ = 60°, c = 26.8/27.6 Å (d = 1.26 g/cm^3)	Fig. 7—bottom

[a] T_t (°C), annealing temperature. All fibers have been annealed for 2.5 h.

107.8°, β = 90.0°, γ = 81.0° accounts for the whole pattern. To fit the experimental density of fiber of about 1.145 g/cm^3, three chains should be accommodated in the unit cell (d_{calcd} = 1.11 g/cm^3). Indeed, especially with regard to the equatorial line, the presence of only few diffraction spots seems not to account for the triclinic hypothesis, which excludes any extinction condition. To make the cell assignment more complicated, crystallites are tilted with respect to the fiber axis direction (Bragg reflections spread out of the layer lines in the diffraction pattern).

According to the X-ray diffraction and thermal analysis, **P**(8) is the only polymer showing a very well-developed crystallinity. This circumstance is not really surprising, taking into consideration the quasi-identical lengths of the flexible and the rigid moieties along the chains (about 10 Å each) which may promote a good rigid–rigid and flexible–flexible register in the molecular packing, as frequently observed for this kind of polymer.

3.2.3. **P***(10)*

The diffraction pattern from virgin fibers shows diffuse peaks at low angle suggesting the appearance of a chain-to-chain register on a large scale which, indeed, is only slightly improved by annealing. The only difference is the enhanced sharpening of the nematic peak at 4.22 Å and the appearance of two more weak but clearly detectable equatorial peaks at 22.0 and 11.0 Å.

3.2.4. **P***(12)*–**P***(14)*

Particularly interesting is the case of **P**(12) and **P**(14) which show mesophases at room temperature with strong meridional reflections (first lattice spacing corresponding to half chain length) and two out of meridian broad reflections on the first and third layer lines. Annealing at very low temperature, compatibly with the thermal stability of the mesophases, leads to a quasi-hexagonal cell containing six chains (a perfect hexagonal packing is confined to the equatorial section of fibers). This resembles very much that observed for **PA**(*n*) [4,16]. Particularly, the extinction of the 00*l* reflections with l = odd suggests the same "bundle" structure that was proposed by us for **PA**(10) [16] on the basis of X-ray diffraction analysis and structure refinement. In this model six chains are packed to give a bundle: three chains at the same level, the other ones translated by (c/2) along z direction, hence the extinction of the odd 00*l* reflections. It is also worth noting the little splitting of the meridional spots probably related to two different chain conformations with a length very close to each other [Δc of about 0.8 Å for both **P**(12) and for **P**(14)] as already reported for LCPs, but of rod-like type [17,18]. Moreover a broad but fairly strong peak is detectable at low angle with lattice spacing 21.4 Å for **P**(12) and 22.1 Å for **P**(14). These spacings are double of those corresponding to the 100 Bragg reflection of the hexagonal phase thus suggesting a very complex supramolecular organization involving a very large number of chains.

4. Conclusion

Hexagonal phases (Hp) have been frequently observed in the case of polymers [19]. It has been shown that, in the case of lateral substituents to the chain backbone of LCPs, Hp phases may be established due to the reciprocal segregation of substituents and chains [16,19–21]. Segregation leads to the organization of several chains in single bundles that pack in a hexagonal array. Generally these phases are partially disordered due to a lack of long range order (LRO) especially in the transverse bundle-to-bundle register. This is the general case of stiff LCPs [21] whereas, in a previous investigation, we have shown that for segmented LCPs [3,16] the LRO is very much enhanced when chain flexibility is increased by increasing the number of methylene units in the flexible spacer. In the case of **P**(*n*) the overall features seem not to perfectly agree with this conclusion probably due to the coupled effect of the statistical *head-to-head* and *head-to-tail* insertion of the allyl–biphenyl unit along the chain and the low melting temperatures which limit the effect of annealing. Of course the shorter axial ratio of the rigid unit of **P**(*n*) must be taken into account, too.

The complex polymorphism and the liquid-crystalline nature of **P**(*n*) makes this class of polymers interesting for drawing a correlation between the phase "structure" and the

occurrence of crosslinking. A report on this topic will appear in a forthcoming article.

Acknowledgements

Support by Ministero dell′Università e della Ricerca Scientifica e Tecnologica in cofinancing this research project is acknowledged (Progetto Nazionale: Sistemi Polimerici per Materiali Compositi). We thank Dr F. De Riccardis for NMR analysis and Mr E. Comunale for the GPC measurements.

References

[1] Di L, Maio LDi, Iannelli P, Pragliola S, Roviello A, Sirigu A. J Polym Sci Part B 1998;36:433.
[2] Caruso U, Iannelli P, Pragliola S, Roviello A, Sirigu A. Macromol Symp 1997;117:43.
[3] Caruso U, Iannelli P, Roviello A, Sirigu A. J Polym Sci Part B 1998;36:2371.
[4] Acierno D, Maio LDi, Iannelli P, Spadaro G, Valenza A. Submitted for publication.
[5] Zentel R, Reckert G. Makromol Chem 1986;187:1915.
[6] Hikmet RAM, Zwerver BH, Lub J. Macromolecules 1994;27:6722.
[7] Kupfer J, Finkelmann H. Makromol Chem Rapid Commun 1991;12:717.
[8] Kundler I, Finkelmann H. Macromol Chem Rapid Commun 1995;16:679.
[9] Shiota A, Ober CK. J Polym Sci Polym Phys 1998;36:31.
[10] Mitchell GR, Davis FJ, Guo W, Cywinski R. Polymer 1991;32:1347.
[11] Remmers M, Dieter N, Wegner G. Makromol Chem Phys 1997;198:2551.
[12] Claisen L, Eisleb O. Liebigs Ann Chem 1913;401:85.
[13] Watanabe J, Krigbaum WR. Macromolecules 1984;17:2288.
[14] Krigbaum WR, Watanabe J, Ishikawa T. Macromolecules 1983;16:1271.
[15] van Luyen D, Strzelecki L. Eur Polym J 1980;16:303.
[16] Acierno D, Maio L Di, Iannelli P. J Polym Sci Part B 1999;37:1601.
[17] Stern R, Ballauff M, Lieser G, Wegner G. Polymer 1991;32:2096.
[18] Liu J, Yuan BL, Geil PH, Dorset DL. Polymer 1997;38:6031.
[19] Ungar G. Polymer 1993;34:2050.
[20] Caruso U, Iannelli P, Pragliola S, Roviello A, Sirigu A. Macromolecules 1995;28:6089.
[21] Watanabe J, Sekine N, Nematsu T, Sone M, Kricheldorf HR. Macromolecules 1996;29:4816.